

Substrate screening effects on the quasiparticle band gap and defect charge transition levels in MoS₂

Mit H. Naik and Manish Jain

*Center for Condensed Matter Theory, Department of Physics,
Indian Institute of Science, Bangalore 560012, India**

Abstract

Monolayer MoS₂ has emerged as an interesting material for nanoelectronic and optoelectronic devices. The effect of substrate screening and defects on the electronic structure of MoS₂ are important considerations in the design of such devices. Here, we present ab initio density functional theory (DFT) and GW calculations to study the effect of substrate screening on the quasiparticle band gap and defect charge transition levels (CTLs) in monolayer MoS₂. We find a giant renormalization to the free-standing quasiparticle band gap by 350 meV and 530 meV in the presence of graphene and graphite as substrates, respectively. Our results are corroborated by recent experimental measurements on these systems using scanning tunneling spectroscopy and photoluminescence excitation spectroscopy. Sulfur vacancies are the most abundant native defects found in MoS₂. We study the CTLs of these vacancies in MoS₂ using the DFT+GW formalism. We find (+1/0) and (0/-1) CTLs appear in the pristine band gap of MoS₂. Substrate screening results in renormalization of the (0/-1) level, with respect to the valence band maximum (VBM), by the same amount as the gap. This results in the pinning of the (0/-1) level about ~500 meV below the conduction band minimum for the free-standing case as well as in the presence of substrates. The (+1/0) level, on the other hand, lies less than 100 meV above the VBM for all the cases.

MoS₂, part of the family of the layered transition metal dichalcogenides (TMDC), has garnered great interest owing to its diverse applications in nanoelectronics and optoelectronics [1–3]. High current on-off ratios in field effect transistors as well as efficient valley and spin control with optical helicity have been achieved using MoS₂[4, 5]. The direct band gap in monolayer MoS₂ is exploited in building ultrasensitive phototransistors [6–8]. MoS₂ is also considered a promising alternative to platinum as a catalyst in the hydrogen evolution reaction [9–11].

Effect of the dielectric environment and defects on the electronic structure of MoS₂ are conceivably the most important considerations in the design of devices using MoS₂ [10, 12–15]. Single layer MoS₂ is typically supported on a substrate. [14, 16–19] This is achieved through transfer post exfoliation or through direct epitaxial growth. [15, 17, 20] Hexagonal boron nitride, graphene, silica and gold are the commonly used substrates. BN is increasingly preferred over SiO₂ since it makes a cleaner interface and minimizes the strain induced in MoS₂. [18, 21] Scanning tunneling spectroscopy (STS) has been used to measure the quasiparticle band gap of MoS₂ on metallic substrates. [17, 22, 23] The screening from the metal is consistently found to reduce the gap. [15–17, 22–25] In the presence of graphene or graphite as substrate, a renormalization larger than 300 meV is observed in the quasiparticle band gap of MoS₂. [15, 17, 25–28] Photoluminescence properties of MoS₂ are also strongly influenced by the ambient dielectric environment. [14, 17, 22, 29]

The most abundant native defect found in monolayer MoS₂ is the sulfur vacancy. [12] The density of naturally occurring sulfur vacancies is about one in a thousand atoms. [12] Sulfur vacancies induce states in the gap of pristine MoS₂, thus affecting its electronic and optical properties. [11, 13, 30–32] While effort is constantly made at attaining lower concentration of defects in MoS₂, sulfur vacancies have found a favourable role in enhancing the rate of hydrogen evolution reaction. [9–11] Due to the induced gap states, hydrogen molecules are found to bind to the bare Mo atom at the sulfur vacancy site. [11] Defect engineering techniques have thus been applied to MoS₂ to increase the density of sulfur vacancies. [11]

A number of theoretical calculations, based on first principles density functional theory (DFT), [33, 34] have been carried out to study sulfur vacancies in monolayer MoS₂. [30, 35–39] These calculations show that the formation energy of the neutral sulfur vacancy is lower than other intrinsic defects in MoS₂. [30, 35, 38] This is in good agreement with experimental findings. [12, 32] Calculation of charged defects and in turn the charge transition levels

(CTLs) within DFT, on the other hand, has pitfalls owing to the underestimation of the band gap in Kohn-Sham DFT. [40] Some simulations use hybrid functionals, as proposed by Heyd, Scuseria and Ernzerhof (HSE), [41] as an attempt to overcome the band gap problem [30, 35]. However, the band gap of monolayer MoS₂ computed using HSE is about 2.2 eV, [30, 35, 42, 43] which is 0.5 eV smaller than the experimentally measured quasiparticle band gap of free-standing MoS₂. [44] This could affect the results on the defect CTLs in MoS₂. Furthermore, the effect of substrate screening on the defect CTLs has not been theoretically explored.

An accurate description of addition or removal of electrons to or from a material is captured using many body perturbation theory (MBPT). MBPT in the GW approximation has been combined with DFT in the well known DFT+GW formalism [45–47] and has been used to predict accurate defect formation energies and CTLs. [48–50] The DFT+GW formalism incorporates atomic relaxations upon adding an electron to the system at the DFT level, and the concomitant quasiparticle excitation at the GW level. Performing GW calculations on transition metal dichalcogenides (TMDCs) are computationally challenging owing to the stringent convergence parameters. [51–53] A DFT+GW study on defects in TMDCs, which entail super cell calculations, require massive computation and has not been attempted yet.

In this letter, we study the effect of substrate screening on the quasiparticle band gap and defect charge transition levels in monolayer MoS₂. We have considered graphene, hexagonal BN, graphite and SiO₂ as substrates. At the DFT level, we find that these substrates do not influence the electronic structure of MoS₂. The DFT band gap of MoS₂ is unchanged in the presence of these substrates. This is due to the absence of long range correlation effects in DFT. At the GW level, however, we find a significant renormalization in the quasiparticle band gap in the presence of these substrates. The quasiparticle gap is renormalized from its free-standing value of 2.74 eV to 2.39 eV in the presence of graphene and to 2.21 eV in the presence of graphite as substrate. In the presence of BN or SiO₂, the gap is close to that of free-standing MoS₂. These results are in good agreement with recent experimental measurements. [15, 17, 23, 44, 54–57] We also study the electronic structure of MoS₂ in the presence of sulphur vacancy defects. The sulfur vacancy induces states in the pristine band gap of MoS₂. We compute the CTLs of the sulfur vacancy using the DFT+GW formalism. Two CTLs appear in the quasiparticle gap: the (+1/0) and (0/-1) levels are 0.1 eV and

2.23 eV above the pristine valence band maximum (VBM), respectively. We further study the effect of substrate screening on the CTLs. The (+1/0) level lies within 100 meV of the VBM in the presence of substrates as well. The (0/-1) level, on the other hand, is pinned \sim 500 meV below the conduction band maximum (CBM), both in the free-standing case as well as in the presence of substrates.

The density functional theory (DFT) calculations are performed using the plane-wave pseudopotential package Quantum Espresso. [58] We use the local density approximation [59] for the exchange correlation functional and norm-conserving pseudopotentials. The wavefunctions are expanded in plane waves upto an energy cut off of 250 Ry. For the unit cell MoS₂ calculations, the cell dimension in the out-of-plane direction is fixed at 35 Å and the Brillouin zone sampled with a 12×12×1 k-point grid. We simulate a sulfur vacancy in MoS₂ by constructing a 5×5 in-plane super cell and removing a sulfur atom. The cell dimension in the out-of-plane direction here is fixed at 18 Å. K-point sampling of 2×2×1 is used in the super cell calculations. The formation energy of charged sulfur vacancies computed at the DFT level need to be corrected for the spurious electrostatic interaction between the charge and its periodic images. The electrostatic corrections are computed using the CoFFEE code. [60]

The quasiparticle excitation energies are computed using the BerkeleyGW code. [61–63] For the unit cell MoS₂ calculation, we use a k-point sampling of 24×24×1 and 8,400 valence and conduction states. We find the quasiparticle band gap of monolayer MoS₂ to be 2.74 eV, which is in good agreement with previous calculations and experimental measurements. [26, 44, 51, 64] Details on the computation of the irreducible polarizabilities of the various substrates is provided in the Supporting Information. For the super cell calculations, we use a k-point sampling of 2×2×1 and 19,000 valence and conduction states. [65, 66] We find that these parameters are sufficient to converge the gap at the *K* point in the Brillouin zone to within 0.2 eV. A dielectric cut off of 35 Ry is used. The Coulomb interaction along the out-of-plane direction is truncated. [67] The dielectric function is extended to finite frequencies using the Hybertsen-Louie generalized plasmon pole (GPP) model. [63]

We study the interaction between MoS₂ and a substrate at the DFT level by constructing commensurate super cells that accommodate the two materials with a strain of less than 2%. We use a 4×4 super cell of MoS₂ and a 5×5 super cell of graphene. Fig. 1 (a) shows the structure of MoS₂ on a graphene substrate. A similar geometry is used for the case

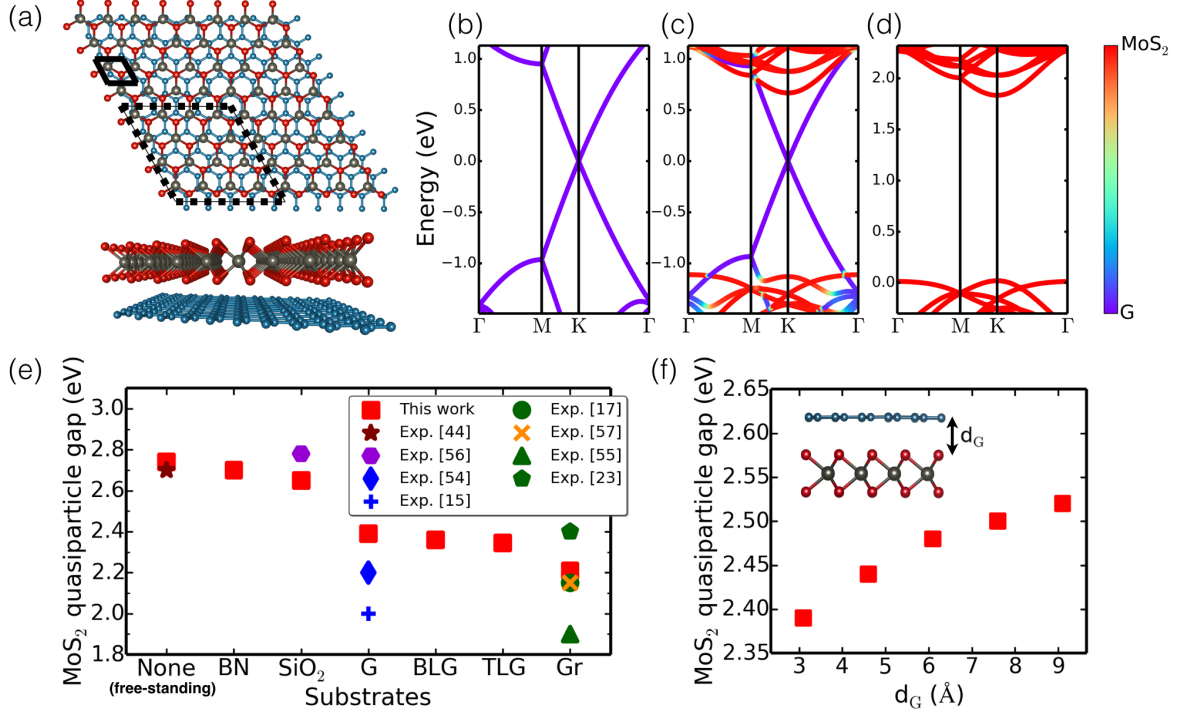


FIG. 1. (a) Single layer MoS₂ on a graphene substrate, top-view and side-view. The black solid line marks the unit cell of MoS₂. The dotted line marks the lattice-matched super cell used to perform the DFT calculations. (b), (c) and (d) DFT band structures of free-standing 5×5 super cell of graphene, lattice matched graphene-MoS₂ heterostructure and free-standing 4×4 super cell of MoS₂, respectively. The colors indicate the projected weights of the heterostructure wavefunctions onto the free-standing layers. (e) Quasiparticle band gap of MoS₂, free-standing, and in the presence of monolayer BN, bulk SiO₂, graphene (G), bilayer graphene (BLG), trilayer graphene (TLG) and graphite substrates. Experimental measurements of the quasiparticle gap in these systems are also shown in the plot. (f) Quasiparticle band gap of MoS₂ in the presence of graphene as a function of increasing inter-layer spacing, d_G .

of MoS₂ on BN (see Supporting Information for more details). The interlayer spacing for the MoS₂-graphene heterostructure is found to be 3.1 Å. Fig. 1 (b) and Fig. 1 (d) show the DFT band structure of the 5×5 super cell of graphene and the 4×4 super cell of MoS₂, respectively. Fig. 1 (c) shows the band structure of the MoS₂-graphene heterostructure. The DFT wavefunction of the heterostructure, for a given band and k-point, has been projected onto the wavefunctions of free-standing graphene and free-standing MoS₂. The projected

weights are then portrayed using a color map. Note that the energy of the VBM have been set to zero in these plots (See Supporting Information for further discussions). It can be seen that interlayer coupling or hybridization is absent at the VBM and CBM of MoS₂ in the heterostructure. At the DFT level, the band gap of MoS₂ in the presence of graphene is unchanged. This is different from bilayer MoS₂ where the overlap of wavefunctions of similar energies leads to strong hybridization and a transition of the gap from direct to indirect [68]. Slight hybridization is, however, seen far from the Fermi level, leading to the creation of small gaps in graphene of about 70 meV. These minigaps have been recently observed in MoS₂-graphene heterostructures using angle-resolved photoemission spectroscopy (ARPES). [69, 70] In the heterostructure, the electronic charge density within each layer is slightly rearranged, but there exists no charge transfer from one layer to the other (See Supporting Information for further discussion).

Performing GW calculations on the various super cell geometries is computationally very demanding. We instead perform separate unit cell calculations on MoS₂ and the substrates. The effect of a substrate on MoS₂ is then taken into account by mapping and adding the irreducible polarizability of the substrate to that of MoS₂. [52, 71, 72]. Using this method, the band gap reduction is slightly overestimated for bulk substrates. Fig. 1e shows the quasiparticle band gap of MoS₂ in the free-standing case and in the presence of BN, SiO₂, graphene (G), bilayer graphene (BLG), trilayer graphene (TLG) and graphite (Gr) substrates. Also marked in the figure are the experimentally measured quasiparticle band gaps of MoS₂ on these substrates. The renormalization in the presence of BN and SiO₂ is 40 meV and 90 meV respectively. In the presence of graphene, BLG, TLG and graphite; the renormalization is 350 meV, 380 meV, 400 meV and 530 meV respectively. Our result for the renormalization in the presence of graphene is in good agreement with a recent GW calculation on the explicit MoS₂-graphene heterostructure. [26] The value of the quasiparticle band gap measured experimentally is in excellent agreement for the free-standing case and in the presence of SiO₂ substrate (Fig. 1e). The experimental quasiparticle band gap of MoS₂ measured in the presence of graphene and graphite substrate, on the other hand, is varied and falls in the range of 1.9 to 2.4 eV (Fig. 1e). We additionally study the effect of MoS₂-graphene interlayer spacing on the quasiparticle band gap of MoS₂. We find that the gap is sensitive to the spacing and can be tuned from 2.39 eV to 2.52 eV (Fig. 1f). We estimate the error in our calculation of the quasiparticle band gap is 100 meV in the case

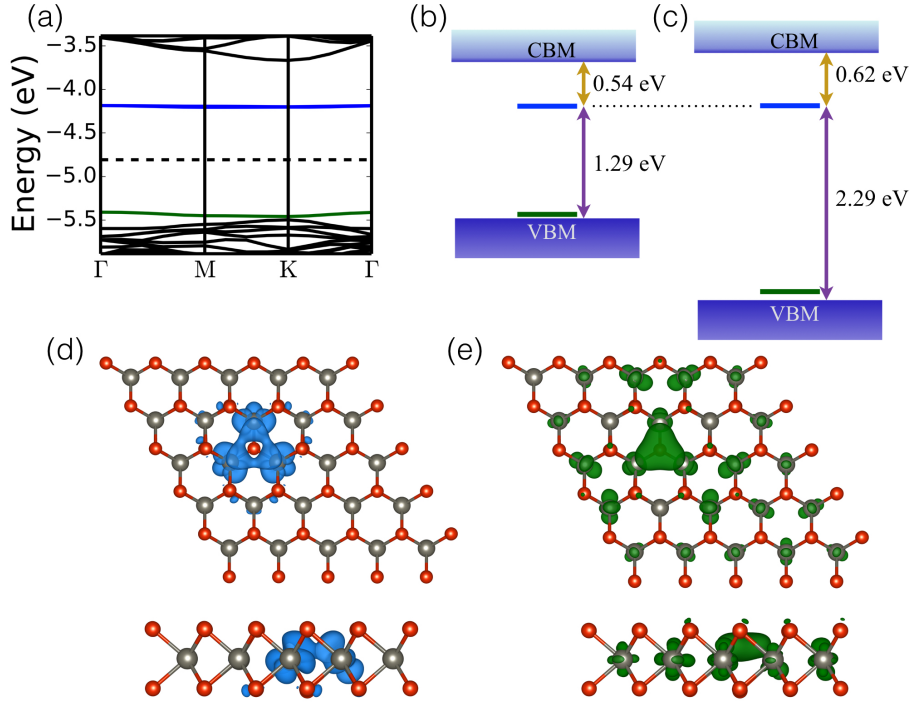


FIG. 2. (a) DFT computed band structure of a sulfur vacancy defect in a 5×5 super cell of MoS_2 . Three defect states are induced in the gap. The filled defect level is indicated in green and the unfilled levels are indicated in blue. The black dashed line marks the Fermi level. (b) Schematic of the DFT pristine VBM, pristine CBM and the defect levels, plotted with respect to the vacuum level. (c) Schematic of the GW pristine VBM, pristine CBM and the defect levels, plotted with respect to the vacuum level. The dotted line is a guide to the eye, showing that the unfilled defect levels line up between DFT and GW levels of theory. (d) and (e) plot the isosurface of the defect levels induced in the gap of MoS_2 . The wavefunction plotted in blue is the corresponding unfilled defect level in the band structure and the one plotted in green is the filled defect level. The top view as well as the side view are shown.

the 2D substrates and 150 meV in the case of bulk substrates. There exist other factors in the experiment that could lead to further renormalization of the band gap in MoS_2 . These include the effect of carrier-induced plasmons in the system, which have recently been shown to close the gap by upto 150 meV. [56, 73] Additional screening from the metallic tip of the scanning tunneling microscope could also further renormalize the band gap. [74]

Fig. 2 (a) shows the DFT band structure of 5×5 super cell of MoS_2 with a sulfur vacancy defect. Three defect states are induced in the gap on introducing the vacancy: one filled

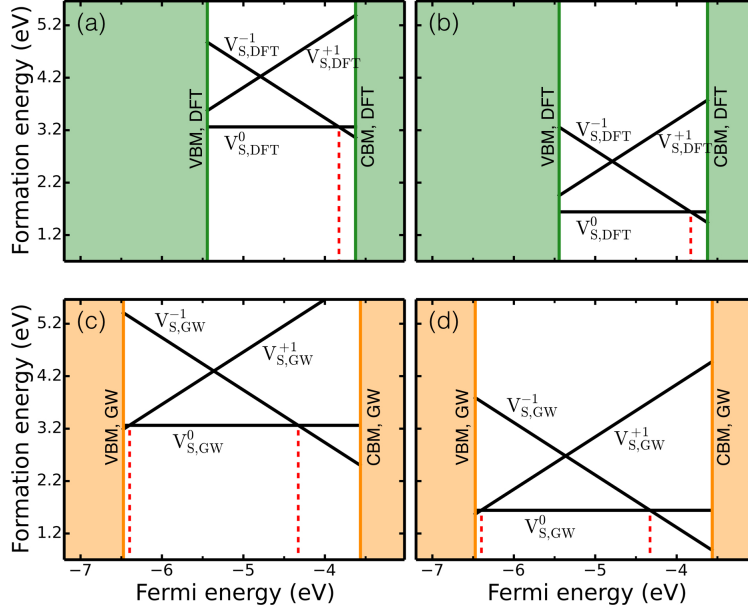


FIG. 3. Formation energy of the sulfur vacancy in different charge states as a function of the Fermi level. The Fermi level is taken to scan the energy range between the pristine VBM and CBM. (a) and (b) Computed at the DFT level, for sulphur rich and sulphur poor conditions respectively. (c) and (d) Computed using the DFT+GW formalism, for sulphur rich and sulphur poor conditions respectively. The charge transition levels that appear in the gap are marked with red dashed lines.

(indicated by green) bonding state and two degenerate unfilled (indicated by blue) anti-bonding states. The charge density associated with these defect states is shown in Fig. 2 (d) and (e). These defect states are dominantly of the Mo- d character (see Supporting Information for partial density of states). The empty states are localised over a smaller region in the material as compared to the filled state. We compare the VBM and CBM of the pristine MoS₂ system, and the defect levels with respect to the vacuum level as computed within DFT and GW. Fig. 2 (b) and (c) shows a schematic of this comparison. We find that the DFT calculated CBM and the GW calculated CBM differ by about 0.1 eV, while the respective VBMs are different by 1 eV. Interestingly, the empty defect levels are found to line up. The filled defect level on the other hand remains shallow and close to the VBM.

The formation energy of a sulfur vacancy in charge state q is given by,

$$E_q^f[\vec{R}_q](E_F) = \{E_q^{\text{tot}}[\vec{R}_q] + E_q^{\text{corr}}\} - E_{\text{pristine}} + q\{\epsilon_{\text{vbm}}^{\text{pristine}} + E_F - \Delta V_{0/p}\} - \mu_S \quad (1)$$

where $E_q^{\text{tot}}[\vec{R}_q]$ refers to the total energy of the 5×5 super cell of MoS₂ containing the defect in charge state q . \vec{R}_q refers to the relaxed atom positions in the super cell of the defect system in charge state q . E_q^{corr} is the electrostatic correction term to redress the spurious interaction of the charged defect with its periodic images. This term is zero for the case of the neutral defect. E_{pristine} is the total energy of a pristine super cell of MoS₂ of the same size. The formation energy is a function of the Fermi level with respect to the VBM of the pristine system, $\epsilon_{\text{vbm}}^{\text{pristine}} + E_F$. $\Delta V_{0/p}$ is the potential alignment term found by comparing the electrostatic potential of the neutral defect cell and pristine cell, far from the defect. μ_S is the chemical potential of the sulfur atom removed from the pristine system to form the vacancy defect. This reference can be chosen to simulate sulfur-rich or sulfur-poor ambient conditions. For the sulfur-rich conditions, the chemical potential is chosen to come from the cyclo-S₈ allotrope of sulfur. Fig. 3 (a) and (b) plot the DFT computed formation energy of the sulfur vacancy in 0, -1 and +1 charge states as a function of the Fermi level. The Fermi level scans the pristine MoS₂ gap. The formation energy here is determined following Eqn. 1 using the DFT computed total energy differences. The electrostatic correction term is determined to be $0.1q^2$ eV, where q is the charge state of the vacancy. Charge transition level, the Fermi level at which the formation energy of one charge state of the defect is equal to that of another is given by:

$$\epsilon^{q/q-1} = E_{q-1}^f[\vec{R}_{q-1}](E_F = 0) - E_q^f[\vec{R}_q](E_F = 0) \quad (2)$$

The only charge transition level stable in the gap at the DFT level is $\epsilon^{0/-1} = 1.62$ eV from the VBM. This is in good agreement with previous calculations [30, 35].

Within the DFT+GW formalism, the expression for the charge transition level can be rewritten into two parts. One that involves adding an electron to the system, and the other that takes into account the lattice relaxation effects due to the added electron [49]. The former is evaluated as a quasiparticle excitation at the GW level and the latter is evaluated at the DFT level.

$$\begin{aligned} \epsilon^{q/q-1} &= (E_{q-1}^f[\vec{R}_{q-1}] - E_{q-1}^f[\vec{R}_q]) + (E_{q-1}^f[\vec{R}_q] - E_q^f[\vec{R}_q]) \\ &= E_{\text{relax}} + E_{\text{QP}} \end{aligned} \quad (3)$$

For the $\epsilon^{0/-1}$ evaluated using the DFT+GW formalism, we find $E_{\text{QP}} = 2.21$ eV and $E_{\text{relax}} = -0.07$ eV. The charge transition level is hence 2.14 eV above the pristine VBM. For the

$\varepsilon^{+1/0}$, we find $E_{\text{QP}} = 0.08$ eV and $E_{\text{relax}} = -0.01$ eV, giving the charge transition level 0.07 eV above the VBM. Fig. 3 (c) and (d) show the plot of formation energy with respect to the Fermi level computed using the DFT+GW formalism. Note that we do not add any electrostatic correction terms here since the quasiparticle excitation energies are taken from the neutral system. The $\varepsilon^{0/-1}$ computed using hybrid functionals in the literature are 1.9 eV [30] and 1.56 eV [35] above the VBM. The $\varepsilon^{+1/0}$ computed using hybrid functionals is found to be below the VBM.

The presence of substrates leads to a renormalization of the pristine quasiparticle band gap in MoS₂ (Fig. 1e), as well as the term E_{QP} in Eqn 3 for the CTL. We compute the renormalization to E_{QP} from the super cell calculation. The renormalization to the pristine band gap, on the other hand, is taken from the unit cell calculations (Fig. 1e). We also assume that the E_{relax} term is the same in the presence and absence of substrates. Fig. 4 shows the CTLs in the quasiparticle band gap of pristine MoS₂ for the various substrates. The $\varepsilon^{+1/0}$ is found to always lie close to the VBM, within 100 meV. The $\varepsilon^{0/-1}$, with respect to the VBM, is renormalized by about the same amount as the band gap. The anti-bonding character of the empty defect states is similar to that of the CBM of the pristine MoS₂ system. [39] The $\varepsilon^{0/-1}$ is thus pinned about 500 meV below the CBM in the presence of substrates as well as in the free-standing configuration. (Fig. 4).

We have studied the effect of substrate screening on the electronic structure of monolayer MoS₂. The substrates included in our calculations are: BN, SiO₂, graphene, bilayer graphene and graphite. These substrates lead to a significant renormalization of the quasiparticle band gap of MoS₂. In the presence of graphene and graphite substrates, in particular, we find a large reduction of 350 meV and 530 meV, respectively. These results are in good agreement with recent experimental measurements on these systems. We have also studied the charge transition levels of sulfur vacancy defects in MoS₂ using the DFT+GW formalism. We find two CTLs lying in the pristine quasiparticle band gap of MoS₂, the (+1/0) and the (0/-1) level. The (+1/0) level and (0/-1) level are found 0.07 eV and 2.14 eV above the pristine VBM, respectively. We have also computed the CTLs in the presence of substrates. We find that, with respect to the VBM, the (0/-1) level is renormalized by the same amount as the gap. The (0/-1) level is thus pinned about 500 meV below the CBM for free-standing MoS₂ case as well as in the presence of substrates. The (+1/0) level, on the other hand, lies less than 100 meV above the VBM in all the cases. A comprehensive understanding of the

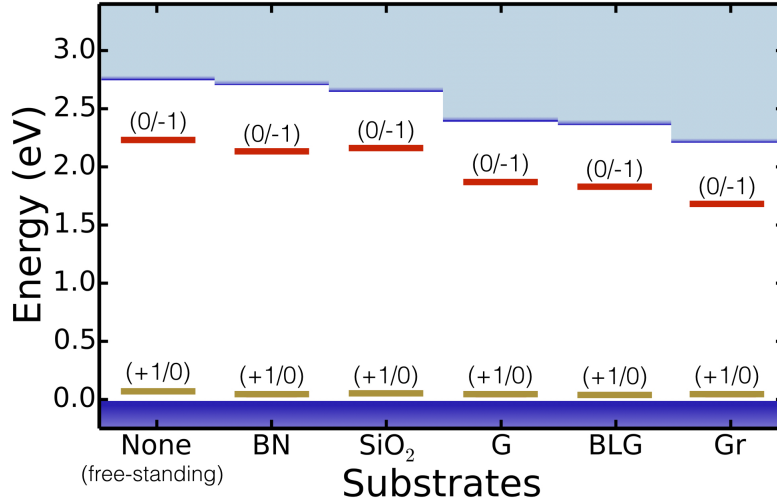


FIG. 4. The $\epsilon^{+1/0}$ and $\epsilon^{0/-1}$ charge transition levels of the sulfur vacancy defect computed using the DFT+GW formalism. The levels are shown with respect to the valence band maximum of pristine MoS₂ in the presence of BN, silica, graphene (G), bilayer graphene (BLG) and graphite (Gr) substrates.

substrate screening effects on the CTLs could aid in choosing substrates for nanoelectronic and optoelectronic devices. It can also open up pathways to effectively tune the properties of MoS₂ through defect and substrate engineering.

We thank the Supercomputer Education and Research Centre (SERC) at IISc for providing the computational facilities. Computational facilities from C-DAC's PARAM Yuva II were also used in this work. We thank Felipe H. da Jornada and Diana Y. Qiu for discussions.

* mjain@iisc.ac.in

- [1] K. F. Mak, C. Lee, J. Hone, J. Shan, and T. F. Heinz, Phys. Rev. Lett. **105**, 136805 (2010).
- [2] A. Splendiani, L. Sun, Y. Zhang, T. Li, J. Kim, C.-Y. Chim, G. Galli, and F. Wang, Nano Letters **10**, 1271 (2010).
- [3] Q. H. Wang, K. Kalantar-Zadeh, A. Kis, J. N. Coleman, and M. S. Strano, Nat Nano **7**, 699 (2012).
- [4] B. Radisavljevic, A. Radenovic, J. Brivio, V. Giacometti, and A. Kis, Nat Nano **6**, 147 (2011).

- [5] K. F. Mak, K. He, J. Shan, and T. F. Heinz, *Nat Nano* **7**, 494 (2012).
- [6] O. Lopez-Sanchez, D. Lembke, M. Kayci, A. Radenovic, and A. Kis, *Nat Nano* **8**, 497 (2013), letter.
- [7] K. Roy, M. Padmanabhan, S. Goswami, T. P. Sai, G. Ramalingam, S. Raghavan, and A. Ghosh, *Nat Nano* **8**, 826 (2013), letter.
- [8] L. Ye, H. Li, Z. Chen, and J. Xu, *ACS Photonics* **3**, 692 (2016), <http://dx.doi.org/10.1021/acsp Photonics.6b00079>.
- [9] D. Voiry, M. Salehi, R. Silva, T. Fujita, M. Chen, T. Asefa, V. B. Shenoy, G. Eda, and M. Chhowalla, *Nano Letters* **13**, 6222 (2013), pMID: 24251828, <http://dx.doi.org/10.1021/nl403661s>.
- [10] K. Chang, Z. Mei, T. Wang, Q. Kang, S. Ouyang, and J. Ye, *ACS Nano* **8**, 7078 (2014), pMID: 24923678, <http://dx.doi.org/10.1021/nn5019945>.
- [11] H. Li, C. Tsai, A. L. Koh, L. Cai, A. W. Contryman, A. H. Fragapane, J. Zhao, H. S. Han, H. C. Manoharan, F. Abild-Pedersen, J. K. Nørskov, and X. Zheng, *Nat Mater* **15**, 48 (2016), letter.
- [12] J. Hong, Z. Hu, M. Probert, K. Li, D. Lv, X. Yang, L. Gu, N. Mao, Q. Feng, L. Xie, J. Zhang, D. Wu, Z. Zhang, C. Jin, W. Ji, X. Zhang, J. Yuan, and Z. Zhang, *Nature Communications* **6**, 6293 EP (2015), article.
- [13] R. Addou, L. Colombo, and R. M. Wallace, *ACS Applied Materials & Interfaces* **7**, 11921 (2015), pMID: 25980312, <http://dx.doi.org/10.1021/acsnano.5b01778>.
- [14] Y. Lin, X. Ling, L. Yu, S. Huang, A. L. Hsu, Y.-H. Lee, J. Kong, M. S. Dresselhaus, and T. Palacios, *Nano Letters* **14**, 5569 (2014), pMID: 25216267, <http://dx.doi.org/10.1021/nl501988y>.
- [15] X. Liu, I. Balla, H. Bergeron, G. P. Campbell, M. J. Bedzyk, and M. C. Hersam, *ACS Nano* **10**, 1067 (2016), pMID: 26565112, <http://dx.doi.org/10.1021/acsnano.5b06398>.
- [16] A. Bruix, J. A. Miwa, N. Hauptmann, D. Wegner, S. Ulstrup, S. S. Grønberg, C. E. Sanders, M. Dendzik, A. Grubišić Čabo, M. Bianchi, J. V. Lauritsen, A. A. Khajetoorians, B. Hammer, and P. Hofmann, *Phys. Rev. B* **93**, 165422 (2016).
- [17] C. Zhang, A. Johnson, C.-L. Hsu, L.-J. Li, and C.-K. Shih, *Nano Letters* **14**, 2443 (2014), pMID: 24783945, <http://dx.doi.org/10.1021/nl501133c>.
- [18] M. K. L. Man, S. Deckoff-Jones, A. Winchester, G. Shi, G. Gupta, A. D. Mohite, S. Kar,

- E. Kioupakis, S. Talapatra, and K. M. Dani, *Scientific Reports* **6**, 20890 EP (2016), article.
- [19] K. Hsieh, V. Kochat, X. Zhang, Y. Gong, C. S. Tiwary, P. M. Ajayan, and A. Ghosh, *Nano Letters* **0**, null (0), pMID: 28786685, <http://dx.doi.org/10.1021/acs.nanolett.7b02099>.
- [20] J. A. Miwa, M. Dendzik, S. S. Gronborg, M. Bianchi, J. V. Lauritsen, P. Hofmann, and S. Ulstrup, *ACS Nano* **9**, 6502 (2015), pMID: 26039108, <http://dx.doi.org/10.1021/acsnano.5b02345>.
- [21] S. Ghatak, S. Mukherjee, M. Jain, D. D. Sarma, and A. Ghosh, *APL Materials* **2**, 092515 (2014), <http://dx.doi.org/10.1063/1.4895955>.
- [22] C.-P. Lu, G. Li, J. Mao, L.-M. Wang, and E. Y. Andrei, *Nano Letters* **14**, 4628 (2014), pMID: 25004377, <http://dx.doi.org/10.1021/nl501659n>.
- [23] Y. L. Huang, Y. Chen, W. Zhang, S. Y. Quek, C.-H. Chen, L.-J. Li, W.-T. Hsu, W.-H. Chang, Y. J. Zheng, W. Chen, and A. T. S. Wee, *Nature Communications* **6**, 6298 EP (2015), article.
- [24] Z. Zhang, X. Ji, J. Shi, X. Zhou, S. Zhang, Y. Hou, Y. Qi, Q. Fang, Q. Ji, Y. Zhang, M. Hong, P. Yang, X. Liu, Q. Zhang, L. Liao, C. Jin, Z. Liu, and Y. Zhang, *ACS Nano* **11**, 4328 (2017), pMID: 28333441, <http://dx.doi.org/10.1021/acsnano.7b01537>.
- [25] S. Ulstrup, A. G. Cabo, J. A. Miwa, J. M. Riley, S. S. Gronborg, J. C. Johannsen, C. Cacho, O. Alexander, R. T. Chapman, E. Springate, M. Bianchi, M. Dendzik, J. V. Lauritsen, P. D. C. King, and P. Hofmann, *ACS Nano* **10**, 6315 (2016), pMID: 27267820, <http://dx.doi.org/10.1021/acsnano.6b02622>.
- [26] C. Jin, F. A. Rasmussen, and K. S. Thygesen, *The Journal of Physical Chemistry C* **119**, 19928 (2015), <http://dx.doi.org/10.1021/acs.jpcc.5b05580>.
- [27] K. T. Winther and K. S. Thygesen, *2D Materials* **4**, 025059 (2017).
- [28] K. Andersen, S. Latini, and K. S. Thygesen, *Nano Letters* **15**, 4616 (2015), pMID: 26047386, <http://dx.doi.org/10.1021/acs.nanolett.5b01251>.
- [29] S. Haastrup, S. Latini, K. Bolotin, and K. S. Thygesen, *Phys. Rev. B* **94**, 041401 (2016).
- [30] J.-Y. Noh, H. Kim, and Y.-S. Kim, *Phys. Rev. B* **89**, 205417 (2014).
- [31] T. L. Atallah, J. Wang, M. Bosch, D. Seo, R. A. Burke, O. Moneer, J. Zhu, M. Theibault, L. E. Brus, J. Hone, and X.-Y. Zhu, *The Journal of Physical Chemistry Letters* **8**, 2148 (2017), pMID: 28448150, <http://dx.doi.org/10.1021/acs.jpcllett.7b00710>.
- [32] W. Zhou, X. Zou, S. Najmaei, Z. Liu, Y. Shi, J. Kong, J. Lou, P. M. Ajayan, B. I. Yakobson, and J.-C. Idrobo, *Nano Letters* **13**, 2615 (2013), pMID: 23659662,

- <http://dx.doi.org/10.1021/nl4007479>.
- [33] W. Kohn and L. J. Sham, *Phys. Rev.* **140**, A1133 (1965).
 - [34] P. Hohenberg and W. Kohn, *Phys. Rev.* **136**, B864 (1964).
 - [35] H.-P. Komsa and A. V. Krasheninnikov, *Phys. Rev. B* **91**, 125304 (2015).
 - [36] S. Halder, H. Vovusha, M. K. Yadav, O. Eriksson, and B. Sanyal, *Phys. Rev. B* **92**, 235408 (2015).
 - [37] D. Le, T. B. Rawal, and T. S. Rahman, *The Journal of Physical Chemistry C* **118**, 5346 (2014), <http://dx.doi.org/10.1021/jp411256g>.
 - [38] S. KC, R. C. Longo, R. Addou, R. M. Wallace, and K. Cho, *Nanotechnology* **25**, 375703 (2014).
 - [39] M. G. Sensoy, D. Vinichenko, W. Chen, C. M. Friend, and E. Kaxiras, *Phys. Rev. B* **95**, 014106 (2017).
 - [40] J. P. Perdew and M. Levy, *Phys. Rev. Lett.* **51**, 1884 (1983).
 - [41] J. Heyd, G. E. Scuseria, and M. Ernzerhof, *The Journal of Chemical Physics* **118**, 8207 (2003), <http://dx.doi.org/10.1063/1.1564060>.
 - [42] S. Bhattacharyya and A. K. Singh, *Phys. Rev. B* **86**, 075454 (2012).
 - [43] J. K. Ellis, M. J. Lucero, and G. E. Scuseria, *Applied Physics Letters* **99**, 261908 (2011), <http://dx.doi.org/10.1063/1.3672219>.
 - [44] N. Krane, C. Lotze, J. M. Lger, G. Reecht, and K. J. Franke, *Nano Letters* **16**, 5163 (2016), pMID: 27459588, <http://dx.doi.org/10.1021/acs.nanolett.6b02101>.
 - [45] P. Rinke, A. Janotti, M. Scheffler, and C. G. Van de Walle, *Phys. Rev. Lett.* **102**, 026402 (2009).
 - [46] M. Hedström, A. Schindlmayr, G. Schwarz, and M. Scheffler, *Phys. Rev. Lett.* **97**, 226401 (2006).
 - [47] C. Freysoldt, B. Grabowski, T. Hickel, J. Neugebauer, G. Kresse, A. Janotti, and C. G. Van de Walle, *Rev. Mod. Phys.* **86**, 253 (2014).
 - [48] A. Malashevich, M. Jain, and S. G. Louie, *Phys. Rev. B* **89**, 075205 (2014).
 - [49] M. Jain, J. R. Chelikowsky, and S. G. Louie, *Phys. Rev. Lett.* **107**, 216803 (2011).
 - [50] W. Chen and A. Pasquarello, *Journal of Physics: Condensed Matter* **27**, 133202 (2015).
 - [51] D. Y. Qiu, F. H. da Jornada, and S. G. Louie, *Phys. Rev. Lett.* **111**, 216805 (2013).
 - [52] A. J. Bradley, M. M. Ugeda, F. H. da Jornada, D. Y. Qiu, W. Ruan, Y. Zhang, S. Wickenburg,

- A. Riss, J. Lu, S.-K. Mo, Z. Hussain, Z.-X. Shen, S. G. Louie, and M. F. Crommie, *Nano Letters* **15**, 2594 (2015).
- [53] D. Y. Qiu, F. H. da Jornada, and S. G. Louie, *Phys. Rev. B* **93**, 235435 (2016).
- [54] J. Shi, M. Liu, J. Wen, X. Ren, X. Zhou, Q. Ji, D. Ma, Y. Zhang, C. Jin, H. Chen, S. Deng, N. Xu, Z. Liu, and Y. Zhang, *Advanced Materials* **27**, 7086 (2015).
- [55] C.-I. Lu, C. J. Butler, J.-K. Huang, C.-R. Hsing, H.-H. Yang, Y.-H. Chu, C.-H. Luo, Y.-C. Sun, S.-H. Hsu, K.-H. O. Yang, C.-M. Wei, L.-J. Li, and M.-T. Lin, *Applied Physics Letters* **106**, 181904 (2015), <http://dx.doi.org/10.1063/1.4919923>.
- [56] K. Yao, A. Yan, S. Kahn, A. Suslu, Y. Liang, E. S. Barnard, S. Tongay, A. Zettl, N. J. Borys, and P. J. Schuck, *Phys. Rev. Lett.* **119**, 087401 (2017).
- [57] M.-H. Chiu, C. Zhang, H.-W. Shiu, C.-P. Chuu, C.-H. Chen, C.-Y. S. Chang, C.-H. Chen, M.-Y. Chou, C.-K. Shih, and L.-J. Li, *Nature Communications* **6**, 7666 EP (2015), article.
- [58] P. Giannozzi, S. Baroni, N. Bonini, M. Calandra, R. Car, C. Cavazzoni, D. Ceresoli, G. L. Chiarotti, M. Cococcioni, I. Dabo, A. D. Corso, S. de Gironcoli, S. Fabris, G. Fratesi, R. Gebauer, U. Gerstmann, C. Gougoussis, A. Kokalj, M. Lazzeri, L. Martin-Samos, N. Marzari, F. Mauri, R. Mazzarello, S. Paolini, A. Pasquarello, L. Paulatto, C. Sbraccia, S. Scandolo, G. Sclauzero, A. P. Seitsonen, A. Smogunov, P. Umari, and R. M. Wentzcovitch, *Journal of Physics: Condensed Matter* **21**, 395502 (2009).
- [59] J. P. Perdew and A. Zunger, *Phys. Rev. B* **23**, 5048 (1981).
- [60] M. H. Naik and M. Jain, *ArXiv e-prints* (2017), arXiv:1705.01491 [cond-mat.mtrl-sci].
- [61] J. Deslippe, G. Samsonidze, D. A. Strubbe, M. Jain, M. L. Cohen, and S. G. Louie, *Computer Physics Communications* **183**, 1269 (2012).
- [62] M. Rohlfing and S. G. Louie, *Phys. Rev. B* **62**, 4927 (2000).
- [63] M. S. Hybertsen and S. G. Louie, *Phys. Rev. B* **34**, 5390 (1986).
- [64] D. Y. Qiu, F. H. da Jornada, and S. G. Louie, *Phys. Rev. Lett.* **115**, 119901 (2015).
- [65] A. Stathopoulos and J. R. McCombs, *ACM Transactions on Mathematical Software* **37**, 21:1 (2010).
- [66] G. Samsonidze, M. Jain, J. Deslippe, M. L. Cohen, and S. G. Louie, *Phys. Rev. Lett.* **107**, 186404 (2011).
- [67] S. Ismail-Beigi, *Phys. Rev. B* **73**, 233103 (2006).
- [68] M. H. Naik and M. Jain, *Phys. Rev. B* **95**, 165125 (2017).

- [69] H. Coy Diaz, J. Avila, C. Chen, R. Addou, M. C. Asensio, and M. Batzill, *Nano Letters* **15**, 1135 (2015), pMID: 25629211, <http://dx.doi.org/10.1021/nl504167y>.
- [70] D. Pierucci, H. Henck, J. Avila, A. Balan, C. H. Naylor, G. Patriarche, Y. J. Dappe, M. G. Silly, F. Sirotti, A. T. C. Johnson, M. C. Asensio, and A. Ouerghi, *Nano Letters* **16**, 4054 (2016), pMID: 27281693, <http://dx.doi.org/10.1021/acs.nanolett.6b00609>.
- [71] M. M. Ugeda, A. J. Bradley, S.-F. Shi, F. H. da Jornada, Y. Zhang, D. Y. Qiu, W. Ruan, S.-K. Mo, Z. Hussain, Z.-X. Shen, F. Wang, S. G. Louie, and M. F. Crommie, *Nat Mater* **13**, 1091 (2014).
- [72] D. Y. Qiu, F. H. da Jornada, and S. G. Louie, *Nano Letters* **0**, null (0), pMID: 28677398, <http://dx.doi.org/10.1021/acs.nanolett.7b01365>.
- [73] Y. Liang and L. Yang, *Phys. Rev. Lett.* **114**, 063001 (2015).
- [74] G. Samsonidze, M. L. Cohen, and S. G. Louie, *Computational Materials Science* **91**, 187 (2014).